Magnetic Resonance Imaging 59 (2019) 114–120

Contents lists available at ScienceDirect

Magnetic Resonance Imaging

journal homepage: www.elsevier.com/locate/mri

Original contribution

Arterial spin-labeling magnetic resonance imaging of brain maturation in early childhood: Mathematical model fitting to assess age-dependent change of cerebral blood flow

Alex Mun-Ching Wong[a,*], Ho-Ling Liu[b], Ming-Lun Tsai[a], Erin Simon Schwartz[c], Chih-Hua Yeh[a], Huei-Shyong Wang[d], Tai-Wei Wu[e], Chien-Yuan Lin[f]

[a] Department of Medical Imaging and Intervention, Chang Gung Memorial Hospital, Keelung/Linkou, and Chang Gung University, Taiwan
[b] Department of Imaging Physics, University of Texas MD Anderson Cancer Center, Houston, TX, USA
[c] Department of Radiology, The Children's Hospital of Philadelphia, Perelman School of Medicine at University of Pennsylvania, Philadelphia, PA, USA
[d] Division of Pediatric Neurology, Department of Pediatrics, Chang Gung Children's Hospital and Chang Gung University, Linkou, Taiwan
[e] Feta and Neonatal Institute, Division of Neonatology, Children's Hospital Los Angeles, Department of Pediatrics, Keck School of Medicine, University of Southern California, Los Angeles, CA, USA
[f] GE Healthcare, Taiwan

ARTICLE INFO

Keywords:
Arterial spin-labeling imaging
Cerebral blood flow
Mathematical model fitting
Akaike information criterion

ABSTRACT

Purpose: To determine the trajectory of age-dependent cerebral blood flow (CBF) change in infants and young children by fitting mathematical models to the imaging data.

Methods: In this retrospective study, we reviewed the arterial spin-labeling imaging studies of 49 typically developing infants and young children at postmenstrual age (PMA) ranging from 38 to 194 weeks. All patients had normal structural MR imaging. Coregistration and gray matter segmentation were performed to extract whole-brain CBF values. Regional CBF values were obtained using manual region-of-interest placement. Curve estimation regression procedures with the corrected Akaike information criterion (AICc) were performed to determine the mathematical model best fitting the relationship between the CBF (whole-brain and regional measurements) and PMA of the patients.

Results: Whole-brain CBF trajectory was best fitted by a cubic model (AICc = 215.95; $R^2 = 0.566$; $P < .001$). Whole-brain CBF at 1, 6, 12, and 24 months was estimated to be 36, 52, 58, and 55 mL/100 g/min, respectively. Regional CBF trajectory was also best fitted by a cubic model in the frontal (AICc = 233.63; $R^2 = 0.442$; $P < .001$), parietal (AICc = 229.18; $R^2 = 0.614$; $P < .001$), basal ganglion (AICc = 239.39; $R^2 = 0.178$; $P = .043$), temporal (AICc = 236.01; $R^2 = 0.441$; $P < .001$), and occipital (AICc = 236.46; $R^2 = 0.475$; $P < .001$) regions.

Conclusions: In early childhood, the trajectory of CBF change was nonlinear and best fitted by the cubic model for the whole brain and all brain regions.

1. Introduction

Brain development is significant in infancy [1] and early childhood. The development involves structural changes including cortical gyration and white matter myelination [1,2], as well as physiological changes that can be assessed by measuring glucose metabolism and cerebral blood flow (CBF) [3,4]. These developmental processes may follow certain patterns or trajectories of change. Non-linear trajectories have been reported in studies evaluating age-related changes of cortical gray matter volume [5] and thickness [6,7] in children. Because gray matter (GM) growth is accompanied by increasing CBF during childhood [8], trajectories of CBF change can also be non-linear and variable. Age-dependent increase in cortical CBF and cerebral glucose utilization in early childhood have been reported, however these studies have employed radioactive nuclear medicine methods such as positron emission tomography or single-photon emission computed tomography [3,9].

Arterial spin-labeling (ASL) perfusion imaging, a noninvasive

* Corresponding author at: Department of Medical Imaging and Intervention, Chang Gung Memorial Hospital, 5 Fu-Hsing Street, Tao Yuan 333, Taiwan.
E-mail addresses: alexmcwchop@yahoo.com (A.M.-C. Wong), hlaliu@mdanderson.org (H.-L. Liu), schwartzES@chop.edu (E.S. Schwartz), wanghs444@adm.cgmh.org.tw (H.-S. Wang), twu@chla.usc.edu (T.-W. Wu).

https://doi.org/10.1016/j.mri.2019.03.016
Received 11 September 2018; Received in revised form 3 March 2019; Accepted 19 March 2019

magnetic resonance (MR) method not requiring the use of a contrast agent or ionizing radiation, has been reported to allow direct measurements of CBF. Using ASL perfusion imaging, age-dependent changes in CBF were investigated in neonates by De Vis et al. [10,11]. Determination of the normal trajectory of CBF change during brain maturation is a prerequisite to the accurate interpretation of CBF measurements in children. Non-linear trajectories of the relationship between age and GM CBF have recently been reported in children aged 6 months to 18 years [12,13]. However, to our knowledge, no studies have systemically evaluated the trajectory of CBF change during brain maturation in infants and young children. In the present study, we measured the CBF in a group of typically developing infants and young children and determined the trajectory of age-dependent CBF change in these patients by systematically fitting mathematical models to the CBF data.

2. Materials and methods

2.1. Patients

Institutional review board approval was obtained for this study. The guardians of all patients provided informed consent before MR examination. Perfusion MR studies performed between 2012 and 2016 of 59 typically developing pediatric patients with normal conventional MR imaging were retrospectively reviewed. The inclusion criteria for this study were (a) age $<$ 3 years and (b) available ASL imaging. The typically developing patients had normal structural MR imaging findings and no developmental abnormalities, neuro-psychiatric disorders, or motor deficits. Indications for clinical MR imaging were varied, as expected from a retrospective analysis, and included transient cyanosis, fever, gait disturbance, hypermelanosis, lethargy, nystagmus, ocular disease, poor feeding, prematurity, scalp hematomas, suspected intracranial vascular lesions, and suspected seizures. Eight patients were excluded because they were subsequently discovered to have a history of cardiopulmonary arrest or were diagnosed with cerebral vascular malformation, encephalitis, meningitis, status epilepticus, or traumatic head injury. Two patients were excluded because their ASL images were degraded by motion artifacts. These criteria were selected in order to exclude patients with known or suspected acute neurologic illness or injury that could affect CBF velocity measurements. Overall, 49 patients [gestational ages at birth (GA): 38 ± 3.19 weeks, and postmenstrual age (PMA): 38 to 194 weeks] were analyzed.

2.2. MR imaging acquisitions

All patients were scanned on a clinical 3T MR imaging scanner (Discovery MR750, GE Healthcare, Milwaukee, WI, USA) with an eight-channel transmit head coil. All MR examinations were performed following oral chloral hydrate administration and, if required, intravenous midazolam. No study was performed under general anesthesia. Conventional images including T1-weighted images (T1WIs), T2-weighted images (T2WIs), fluid-attenuated inversion recovery images, and diffusion-weighted images were obtained.

ASL imaging was performed using a pseudocontinuous ASL (PCASL) sequence with a three-dimensional (3D) background-suppressed fast-spin-echo stack-of-spiral readout module with eight in-plane spiral interleaves (TR/TE = 4463 ms/10.2 ms, labeling duration = 1500 ms, postlabeling delay = 1525 ms for children and 2025 ms for neonates, in-plane matrix = 128 × 128, number of excitations = 3, field of view = 240 mm × 240 mm, slice thickness = 5 mm) and an echo train length of 23 to obtain 23 consecutive axial slices. The labeling plane was 10 mm thick and was placed 20 mm inferior to the lower edge of the cerebellum. The PCASL scan also included the acquisition of a reference image after saturation recovery with a saturation time of 2 s. The total scan time was 4 min 19 s.

2.3. Data analysis

ASL perfusion data were analyzed with Matlab 7.8 (The MathWorks, Inc., Natick, MA, USA). The CBF was calculated using a simplified model [14] with the following assumptions: T1 of blood = 1.6 s, partition coefficient = 0.9, and overall efficiency = 0.6 [product of labeling efficiency (0.80) and background suppression (0.75)]. ASL perfusion images were visualized and analyzed by an experienced pediatric neuroradiologist with 7 years of experience in ASL imaging, using Mango (Research Imaging Institute, University of Texas Health Science Center, San Antonio, TX, USA). The perfusion images were reviewed to ensure both a normal brain perfusion pattern and a perfusion symmetry. In infancy, the brain perfusion pattern was considered normal if the CBF decreased in the expected order: that is highest in the basal ganglia and thalami, then the cerebral cortex, and lowest in the cerebral white matter [11,15]. The perfusion pattern was interpreted as abnormal if a region demonstrating a visibly different color from that of the majority of the brain was present on the color-coded CBF maps. The perfusion was interpreted as symmetrical if no color mismatch was observed between the two cerebral hemispheres.

2.4. Gray matter CBF calculation

2.4.1. Whole-brain CBF calculation

Using SPM8 (http://www.fil.ion.ucl.ac.uk/spm), we coregistered the T1-weighted image set of each subject to the UNC Infant 0-1-2 Atlases templates [16], and segmented the images into gray matter (GM) probability maps. By using Mango, pixels with GM probability $>$ 0.8 of the GM maps were used to create GM masks. These GM masks were then coregistered to the control images of the ASL data set using SPM8 to create GM-ASL masks, which were transformed to GM-ASL region-of-interest (ROI) sets using Mango. Cerebral GM-ASL ROI sets were created by manually excluding the ROI covering the brainstem and the cerebellum from the GM-ASL ROI sets. For each of the ASL perfusion calculations, the cerebral GM-ASL ROIs, placed on the corresponding ASL-CBF images (Fig. 1A and B), were used to extract GM-CBF values. These GM-CBF values were averaged to obtain a whole-brain GM-CBF value for each patient.

2.4.2. Regional CBF calculation

Using Mango, two operators separately drew regional ROIs of the basal ganglia, frontal, parietal, temporal, and occipital regions on the corresponding ASL-CBF images (Fig. 1C–E) to calculate the regional CBF values for each subject. The ROIs were carefully drawn to minimize the partial-volume effects of the CBF measurements. After a consensus was reached on the anatomical localization of the ROIs by the two operators, the CBF values were obtained from these ROIs. The CBF values from the left and right hemispheres were combined to obtain an average CBF value for each region.

2.5. Statistical analysis

Curve estimation regression procedures were performed to determine the best-fitting mathematical model to describe the relationship between the CBF (whole brain and regional measurements) and the PMA of the patients. Common regression models (linear, logarithmic, quadratic, cubic, power, and exponential) were fitted to the data by using SPSS (version 22.0; IBM, Armonk, NY, USA), and the first order kinetic model [17] was fitted to the data by using Sigma Plot (version 13; Systat Software Inc., San Jose, CA, USA) to determine the coefficient of determination (R^2) and statistical significance of each model. A P value of < 0.05 was considered statistically significant.

We compared the models by using the corrected Akaike information criterion (AICc) to select the best-fit model [18–20]. The AICc calculations of the common models were performed with XLSTAT add-on software (XLSTAT version 2017, Addinsoft, USA) in Microsoft Excel

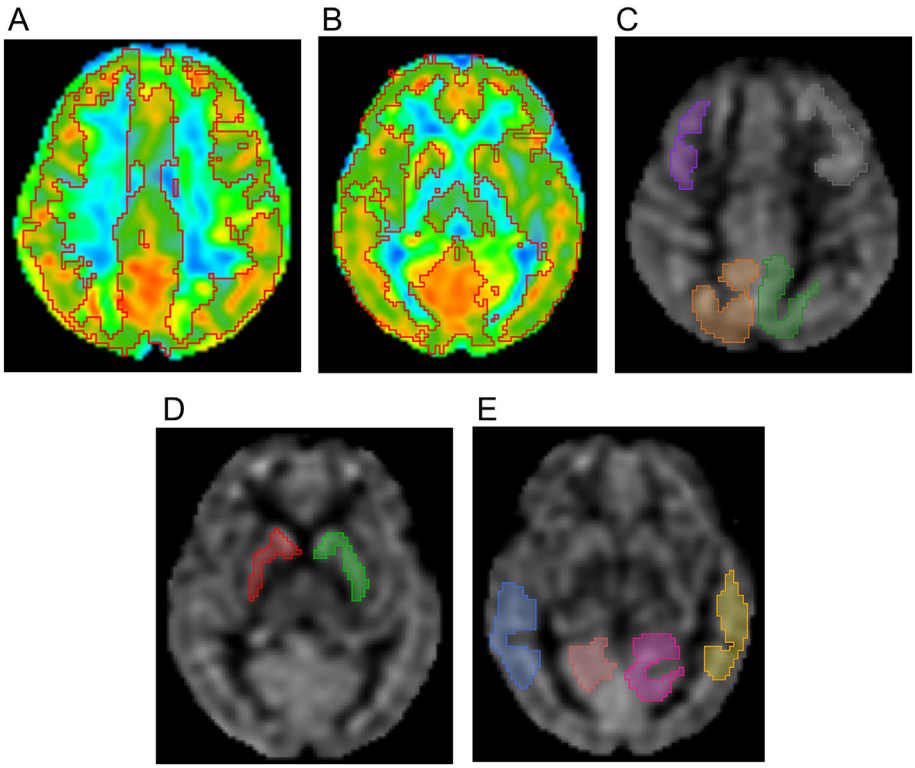

Fig. 1. Representative images of a baby girl born at 40 weeks postmenstrual age (PMA) and scanned at 99 weeks PMA. Whole-brain cerebral blood flow (CBF) was measured, after coregistration and segmentation of brain images to create gray matter regions-of-interest (ROI) on ASL perfusion images (A, B), with representative images shown at levels of the centrum semiovale and the basal ganglia. Regional CBF was measured with ROIs placed in the frontal and parietal regions (C), the basal ganglia (D), and the temporal and occipital regions (E).

2013 (Microsoft, WA, USA) and the AICc calculation of the first order kinetic model was performed on Sigma Plot (version 13). The model with the smallest AICc value was selected as the best regression with PMA of that measurement. The Akaike information criterion (AIC) is a method of model selection that compares non-nested models while penalizing for model complexity [20]. The AIC has been modified as AICc to correct for bias in small-sample application [18]. AICc is defined as $AIC + 2K \times (K + 1) / (N - K - 1)$, and AIC as $N \times \ln(RSS) + 2K$, where K is the number of parameters in the model, N is the number of data points, and RSS is the residual sum of squares.

3. Results

3.1. Whole-brain analysis

The graph of correlation between whole-brain CBF and PMA revealed that the CBF increased with increasing PMA before 90 weeks, plateaued from 90 to 160 weeks, and increased with increasing PMA thereafter (Fig. 2). The best-fitting model was the cubic model (AICc = 215.95; $R^2 = 0.566$; $P < .001$), followed by the logarithmic (AICc = 222.06; $R^2 = 0.448$; $P < .001$) and the power (AICc = 223.37; $R^2 = 0.440$; $P < .001$) models. (Table 1 and Supplementary Tables 1 and 2). According to the cubic model, whole-brain CBF at 1, 6, 12, and 24 months was estimated to be 36, 52, 58, and 55 mL/100 g/min, respectively (Fig. 2 and Table 2).

3.2. Regional CBF analysis

The graphs of the correlation between CBF and PMA in the frontal, parietal, basal ganglia, temporal, and occipital regions all showed that the CBF increased with increasing PMA before 90 weeks, plateaued from 90 to 160 weeks, and increased with increasing PMA thereafter (Fig. 3). The cubic model was the best-fitting model for the frontal (AICc = 233.63; $R^2 = 0.442$; $P < .001$), parietal (AICc = 229.18; $R^2 = 0.614$; $P < .001$), basal ganglion (AICc = 239.39; $R^2 = 0.178$; $P = .043$), temporal (AICc = 236.01; $R^2 = 0.441$; $P < .001$), and occipital (AICc = 236.46; $R^2 = 0.475$; $P < .001$) regions. The CBF at 1, 6, 12, and 24 months, estimated according to the best-fitting model for each brain region, is presented in Table 2.

4. Discussion

Our results showed that the cubic model was the best-fitting model (AICc = 215.95; $R^2 = 0.566$; $P < .001$) for the regression between whole-brain CBF and PMA. In this model, whole-brain CBF increased with increasing PMA before 90 weeks, plateaued from 90 to 160 weeks, and increased with increasing PMA thereafter (Fig. 2). The trend of the correlation between age and CBF was positive for all mathematical models. For regional CBF measurements, the best-fitting models for various regions are listed in Table 1, with the cubic model for all cerebral cortical regions ($R^2 = 0.441–0.614$, $P < .001$). For the basal ganglia, the best-fitting model was the cubic model, but with an exceptionally low R^2 (0.178; $P = .043$). The cubic model was characterized by an initial rapid increase, followed by a slow increase or plateau, and finally a rebound. The rapid increase in CBF within the first year of age (PMA = 90 weeks) agreed with the results of a longitudinal study of CBF measurements over the first 30 months [21], in which a considerable increase in CBF was noted during the first 6 months and followed by a slow increase in CBF until approximately 24 months. This considerable increase in perfusion during infancy may reflect physiological and structural changes of the brain during maturation, including glucose consumption, myelination, and gray matter volume change [21]. Cerebral glucose consumption can increase with age during maturation in infancy and early childhood [4,22]. Increased neural synaptic density and intracortical myelination have been observed during maturation [23]. Nonlinear trajectories of gray matter volume change were initially reported by Giedd et al. [5] and further reported by Shaw et al. to show cubic and quadratic trajectories in high-order association cortical areas [7]. Studies have demonstrated positive correlations between CBF and factors, namely brain glucose consumption [24] and synaptic density or myelination [22] in children, therefore contributing toward increased perfusion. The different phases of the cubic curve in

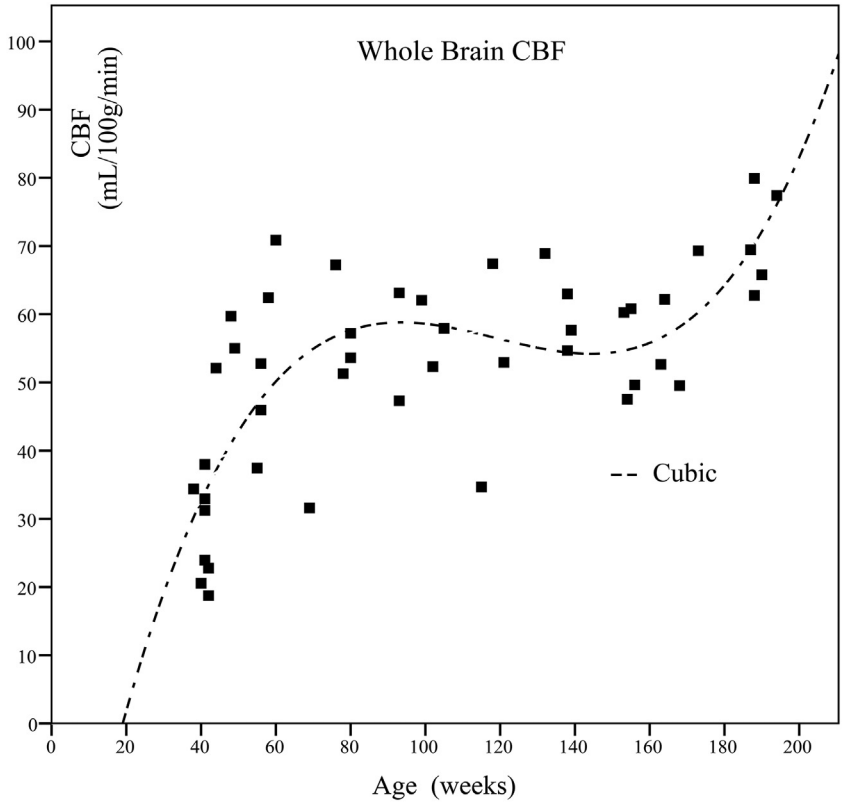

Fig. 2. Graph of whole-brain cerebral blood flow as a function of postmenstrual age in weeks. The line represents the correlation adopting the best-fitting mathematical model.

infancy and early childhood could be explained by different rates of these maturational processes. Studies have reported an increasing trend of CBF with age in infants [9,10]. By using pulsed ASL imaging, two studies have reported CBF in children aged through 6 months to 18 years and assessed the trajectory of age-related CBF change through mathematical modeling [12,13]. However, with a focus on the period of infancy and early childhood, the trajectory of CBF change during maturation has not been investigated through ASL perfusion imaging. Therefore, we performed modeling of CBF changes with PMA to determine the best-fitting model for CBF change during infancy and early childhood. Formulas were generated to enable prediction of CBF based on PMA. Moreover, the widely recommended ASL perfusion sequence, the PCASL sequence with 3D readout and background suppression [14], was employed to measure the CBF of our subjects.

The trends of perfusion changes with respect to age have been reported in different brain regions in neonates and infants. In the neonatal period, relative CBF can exhibit a 5%–30% increase in the frontal regions and a 25%–50% increase in the occipital regions, but a 3%–40% decrease in the basal ganglia and thalami [4,10]. Using Xenon-enhanced computed tomography (CT) to measure perfusion changes within the first 6 months of infancy, Chiron et al. reported a 10% and 8% increase of relative CBF in the frontal and occipital regions, respectively, but a 12% decrease in the thalamus. Our results revealed an 11% and 16% increase of CBF in the frontal and occipital regions, respectively, in the neonatal period, and a 27% and 44% increase in the frontal and occipital regions, respectively, in 2–6 months of PMA (Fig. 3

Table 2
Cerebral blood flow (mL/100 g/min) of brain regions at postnatal ages in months (postmenstrual age in weeks) of 1 (43), 6 (65), 12 (91), and 24 (144) estimated according to the best-fitting model.

Age	WB	Frontal	Parietal	BG	Temporal	Occipital
1 m	36	41	35	49	40	43
6 m	52	58	59	62	57	62
12 m	58	65	67	63	67	69
24 m	55	61	59	52	60	63

WB denotes whole-brain and BG basal ganglia.

Table 1
Mathematical model fitting of regression between the cerebral blood flow (mL/100 g/min) and postmenstrual age (weeks) in the whole brain and other brain regions.

Region	Top 3 well-fitted models (best-fitted)	Best-fitting model			
		AICc	R^2	*P*	Regression
Whole brain	Cubic, Log, power	215.954	0.566	< .001	$Y = -45.64 + 2.85X - .025X^2 + 7.04 * 10^{-5}X^3$
Frontal	Cubic, Log, first order kinetic	233.634	0.442	< .001	$Y = -36.93 + 2.71X - .023X^2 + 6.32 * 10^{-5}X^3$
Parietal	Cubic, Log, first order kinetic	229.176	0.614	< .001	$Y = -80.92 + 3.94X - .034X^2 + 9.17 * 10^{-5}X^3$
Basal ganglion	Cubic, first order kinetic, Log	239.393	0.178	.043	$Y = -21.49 + 2.55X - .024X^2 + 6.73 * 10^{-5}X^3$
Temporal	Cubic, first order kinetic, power	236.009	0.441	< .001	$Y = -44.57 + 2.87X - .024X^2 + 6.37 * 10^{-5}X^3$
Occipital	Cubic, first order kinetic, Log	236.462	0.475	< .001	$Y = -50.26 + 3.21X - .028X^2 + 7.57 * 10^{-5}X^3$

In each region, the models are listed with R^2, *P* value and estimated equations with X denoting postmenstrual age and Y denoting the CBF. Log denotes logarithmic and AICc corrected Akaike information criterion.

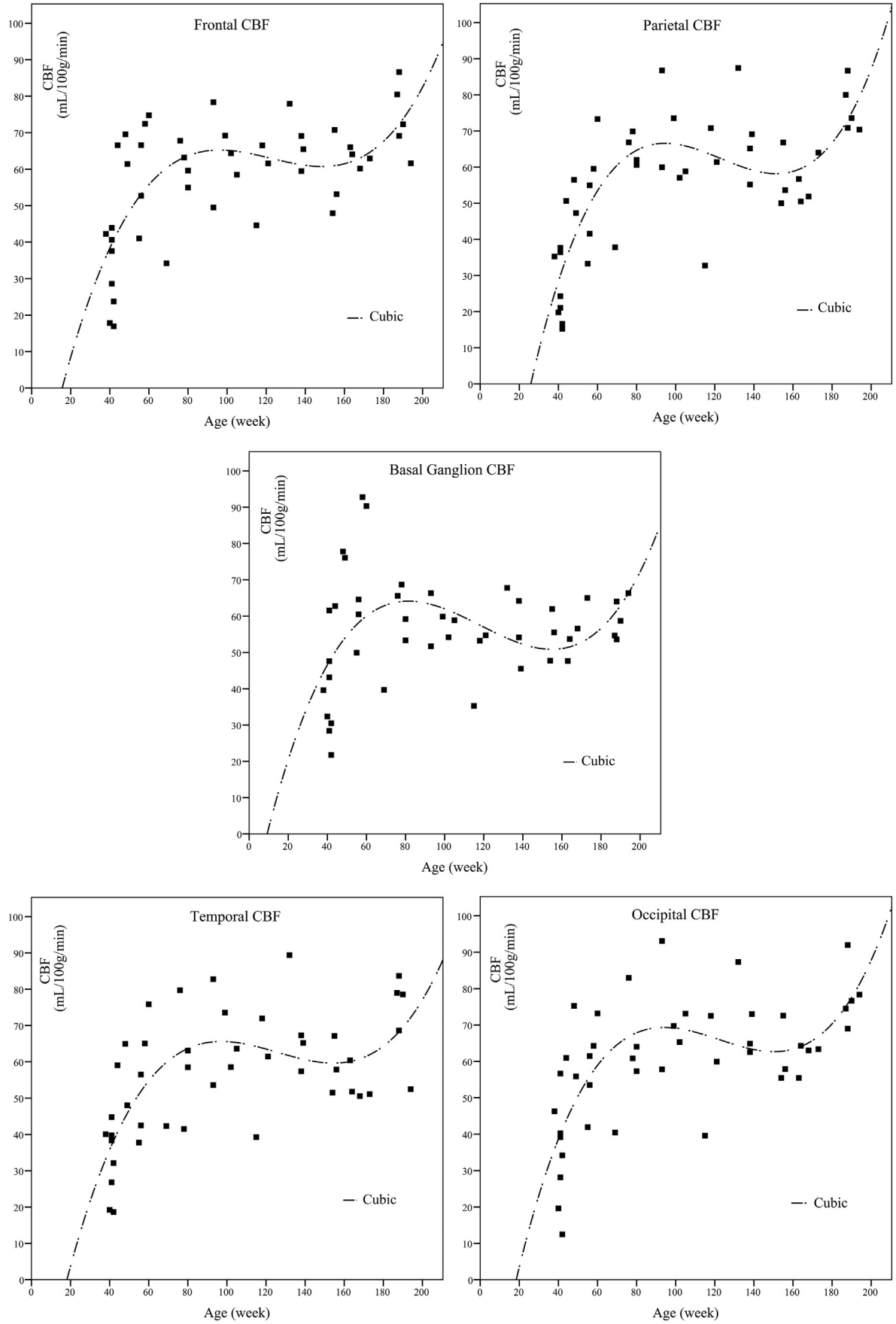

Fig. 3. Graphs of regional cerebral blood flow as a function of postmenstrual age in weeks in the frontal, parietal, basal ganglia, temporal, and occipital regions. In each graph, the line represents the correlation adopting the best-fitting mathematical model.

and Table 2). However, unlike previous reports, our results did not reveal a decrease of CBF in the basal ganglia; rather, a 9% increase of CBF was observed in the basal ganglia in the neonatal period and a 27% increase during 2–6 months of PMA (Fig. 3). These discrepancies may be attributed to the underlying differences between our and previous studies. First, we reported the absolute CBF instead of normalizing the regional CBF measurements to those of other regions. Normalization of the CBF in the brain regions to the whole-brain CBF not only reduced the individual variations, but also largely reduced, if not eliminated, the effect of age-related maturational change on the CBF (Supplementary Fig. 1 and Supplementary Table 3). Absolute CBF quantification by using ASL imaging may thus capture important information of CBF measurement, such as age-related variations. Furthermore, the vascularized basal ganglia may be subject to variable contribution of the vascular signal during perfusion measurement [11], reducing the reliability of CBF measurement using ASL imaging. Unlike the neonatal study reported by De Vis et al. [11], our study investigated a population comprising neonates, infants, and young children, the trajectory results were based on mathematical fitting of the data obtained from all patients and not only from the neonates. Moreover, only common models were selected to fit the CBF measurements in our study, a more complicated model that better fit the measurements may exist that was not selected for our analysis. These features may also explain the low coefficient (R^2) of the cubic model fitting the regional CBF measurements in the basal ganglia.

Knowledge of reference CBF values and age-related changes is essential to interpreting perfusion imaging results. However, only a few studies have reported CBF values of the whole brain in the neonatal period and during early infancy. In the neonatal period, whole-brain CBF has been reported to range from 21 to 29 mL/100 g/min by using ASL perfusion imaging [11,25] and approximately 50 mL/100 g/min by using Xenon-enhanced CT [9]. Our study revealed a whole-brain CBF value of 36 mL/100 g/min, estimated from the cubic curve as the best-fitting model for the data (Fig. 2 and Supplementary Table 1), and our results were in line with those obtained by ASL perfusion studies. The lower CBF values measured with ASL imaging, when compared with those measured with Xenon-enhanced CT, may be explained by the intrinsically low signal-to-noise ratio of the neonatal brain on ASL imaging [11]. Notably, while both previous ASL studies have not mentioned how the whole-brain CBF values were calculated, we measured the whole-brain CBF with ROIs created through coregistration of images to neonatal templates [16] and segmentation of gray matter.

Quantification of CBF by using ASL imaging requires mathematical modeling, practically adopting assumed adult parameters, may affect the accuracy of CBF quantification in neonates. Perfusion inaccuracies in neonates may arise from adopting age-related parameters including the T1 of blood (T1b) and the blood-brain partition coefficient of water (λ) [26], because neonates have a longer T1b [26,27] and higher λ [26,28] than adults have. However, simulation studies in neonates using adult values of T1b have resulted in CBF overestimation by approximately 10% [26,29], with adult values of λ causing a 5% CBF underestimation of CBF [26,28], leading to a combined 5% CBF overestimation if adopting both sets of adult parameters. Incorporating developmental changes in other physiological parameters, such as the T2 of blood, T1 and T2 of brain tissue, and equilibrium blood magnetization, has a negligible effect on CBF quantification [30,31].

Studies have addressed the effect of midazolam sedation on CBF. In a study including 10 very-low-birthweight infants on ventilator, mean CBF measured by transcranial Doppler ultrasound decreased from baseline by 12% at 5 min before returning to predose values, suggesting a transient effect of sedation on CBF [32]. A recent study of 100 healthy children aged 4 months to 18 years reported no significant CBF differences in any brain regions between sedated ($n = 7$, mean age = 7.6 years) and non-sedated ($n = 4$, mean age = 7.9 years) children [8]. We therefore believed that sedation should not substantially alter CBF, and even if sedation mildly reduced CBF in the present study, the effect should have been transient enough to not significantly affect our results.

The clinical implications of the present study should be emphasized. We reported the CBF data of typically developing patients including neonates, infants, and young children obtained through ASL perfusion imaging. Our results can serve as a reference for interpreting CBF data given that only a few studies have focused on the perfusion of children within these age groups [9,11,25]. More importantly, we investigated the relationship between CBF and age in these children by assessing the goodness of fit of the mathematical models to the perfusion data. By combining the information theory and the maximum likelihood theory, the AIC is an estimator for model selection that balances the goodness of fit and the complexity of the tested model [20]. In our study, the corrected AIC, a modified version of the AIC more accurate in model selection for finite sample sizes [18,19], was used to select the best-fitting model for the age-related CBF change. Although age-related changes of CBF in neonates and infants have been studied previously, most studies have assumed a linear relationship of the CBF change. The current study is a preliminary step toward further investigation of maturation changes, which requires confirmation in a larger series and among children in other age ranges.

The limitations of this study include inclusion of typically developing patients, rather than healthy volunteers, because typically developing patients were more readily available. However, these typically developing patients were imaged under clinical settings similar to those of most patients in daily clinical practice; this thus produced a more clinically generalizable experience. An additional limitation was that our GM CBF measurements may have been affected by partial-volume effects, although the effects would be less obvious on the regional CBF measurements (using manual ROI placement) than on the whole-brain CBF measurement. Finally, our study was a cross-sectional retrospective study. Although difficult to perform, a cohort study would be more appropriate to investigate the longitudinal age-related CBF change in each subject in order to reduce inter-subject variation.

5. Conclusion

By using mathematical model fitting, we determined the trajectory of the age-related CBF change in a group of typically developing infants and toddlers. The cubic model was the best-fitting trajectory of the age-related CBF change for the whole brain and for all brain regions. Generated formulas from our results can be employed to estimate the CBF using the PMA of typically developing children within the aforementioned age range.

Supplementary data to this article can be found online at https://doi.org/10.1016/j.mri.2019.03.016.

Declaration of conflicting interests

The authors declare no conflict of interest.

Acknowledgment

The authors thank Mr. Morris MF Wu for providing advice on statistical analysis.

Funding

This study was partly supported by the Ministry of Science and Technology, Taiwan (grant numbers NSC 102-2314-B-182A-097; MOST 103-2314-B-182A-008, MOST 104-2314-B-182A-093, MOST 106-2314-B-182A-015).

References

[1] Provenzale JM, Liang L, DeLong D, White LE. Diffusion tensor imaging assessment of brain white matter maturation during the first postnatal year. AJR Am J Roentgenol 2007;189(2):476–86.

[2] Dubois J, Benders M, Borradori-Tolsa C, Cachia A, Lazeyras F, Ha-Vinh Leuchter R, et al. Primary cortical folding in the human newborn: an early marker of later functional development. Brain: a journal of neurology 2008;131(Pt 8):2028–41.
[3] Chugani HT, Phelps ME. Maturational changes in cerebral function in infants determined by 18FDG positron emission tomography. Science (New York, NY) 1986;231(4740):840–3.
[4] Kinnala A, Suhonen-Polvi H, Aarimaa T, Kero P, Korvenranta H, Ruotsalainen U, et al. Cerebral metabolic rate for glucose during the first six months of life: an FDG positron emission tomography study. Arch Dis Child Fetal Neonatal Ed 1996;74(3):F153–7.
[5] Giedd JN, Blumenthal J, Jeffries NO, Castellanos FX, Liu H, Zijdenbos A, et al. Brain development during childhood and adolescence: a longitudinal MRI study. Nat Neurosci 1999;2(10):861–3.
[6] Ducharme S, Albaugh MD, Nguyen TV, Hudziak JJ, Mateos-Perez JM, Labbe A, et al. Trajectories of cortical thickness maturation in normal brain development–the importance of quality control procedures. Neuroimage 2016;125:267–79.
[7] Shaw P, Kabani NJ, Lerch JP, Eckstrand K, Lenroot R, Gogtay N, et al. Neurodevelopmental trajectories of the human cerebral cortex. J Neurosci 2008;28(14):3586–94.
[8] Forkert ND, Li MD, Lober RM, Yeom KW. Gray matter growth is accompanied by increasing blood flow and decreasing apparent diffusion coefficient during childhood. AJNR Am J Neuroradiol 2016;37(9):1738–44.
[9] Chiron C, Raynaud C, Maziere B, Zilbovicius M, Laflamme L, Masure MC, et al. Changes in regional cerebral blood flow during brain maturation in children and adolescents. Journal of nuclear medicine: official publication, Society of Nuclear Medicine 1992;33(5):696–703.
[10] De Vis JB, Hendrikse J, Bhogal A, Adams A, Kappelle LJ, Petersen ET. Age-related changes in brain hemodynamics; a calibrated MRI study. Hum Brain Mapp 2015;36(10):3973–87.
[11] De Vis JB, Petersen ET, de Vries LS, Groenendaal F, Kersbergen KJ, Alderliesten T, et al. Regional changes in brain perfusion during brain maturation measured non-invasively with arterial spin labeling MRI in neonates. Eur J Radiol 2013;82(3):538–43.
[12] Taki Y, Hashizume H, Sassa Y, Takeuchi H, Wu K, Asano M, et al. Correlation between gray matter density-adjusted brain perfusion and age using brain MR images of 202 healthy children. Hum Brain Mapp 2011;32(11):1973–85.
[13] Carsin-Vu A, Corouge I, Commowick O, Bouzille G, Barillot C, Ferre JC, et al. Measurement of pediatric regional cerebral blood flow from 6 months to 15 years of age in a clinical population. Eur J Radiol 2018;101:38–44.
[14] Alsop DC, Detre JA, Golay X, Gunther M, Hendrikse J, Hernandez-Garcia L, et al. Recommended implementation of arterial spin-labeled perfusion MRI for clinical applications: a consensus of the ISMRM perfusion study group and the European consortium for ASL in dementia. Magn Reson Med 2015;73(1):102–16.
[15] Biagi L, Abbruzzese A, Bianchi MC, Alsop DC, Del Guerra A, Tosetti M. Age dependence of cerebral perfusion assessed by magnetic resonance continuous arterial spin labeling. J Magn Reson Imaging 2007;25(4):696–702.
[16] Shi F, Yap PT, Wu G, Jia H, Gilmore JH, Lin W, et al. Infant brain atlases from neonates to 1- and 2-year-olds. PloS one 2011;6(4):e18746.
[17] Gomez M, Murcia MD, Gomez E, Ortega S, Sanchez A, Thaikovskaya O, et al. Modelling and experimental checking of the influence of substrate concentration on the first order kinetic constant in photo-processes. J Environ Manage 2016;183(Pt 3):818–25.
[18] Hurvich CM, Tsai CL. Bias of the corrected AIC criterion for UNDERFITTED regression and time-series models. Biometrika 1991;78(3):499–509.
[19] Cavanaugh JE. Unifying the derivations for the Akaike and corrected Akaike information criteria. Stat Probab Lett 1997;33(2):201–8.
[20] Akaike H. A new look at the statistical model identification. Automatic Control, IEEE Transactions on 1974;19(6):716–23.
[21] Kehrer M, Schoning M. A longitudinal study of cerebral blood flow over the first 30 months. Pediatr Res 2009;66(5):560–4.
[22] Chugani HT. A critical period of brain development: studies of cerebral glucose utilization with PET. Prev Med 1998;27(2):184–8.
[23] Huttenlocher PR. Synaptic density in human frontal cortex - developmental changes and effects of aging. Brain Res 1979;163(2):195–205.
[24] Fox PT, Raichle ME, Mintun MA, Dence C. Nonoxidative glucose consumption during focal physiologic neural activity. Science 1988;241(4864):462–4.
[25] Miranda MJ, Olofsson K, Sidaros K. Noninvasive measurements of regional cerebral perfusion in preterm and term neonates by magnetic resonance arterial spin labeling. Pediatr Res 2006;60(3):359–63.
[26] Wang J, Licht DJ. Pediatric perfusion MR imaging using arterial spin labeling. Neuroimaging Clin N Am 2006;16(1):149–67. [ix].
[27] Varela M, Hajnal JV, Petersen ET, Golay X, Merchant N, Larkman DJ. A method for rapid in vivo measurement of blood T1. NMR Biomed 2011;24(1):80–8.
[28] Varela M, Petersen ET, Golay X, Hajnal JV. Cerebral blood flow measurements in infants using look-locker arterial spin labeling. J Magn Reson Imaging 2015;41(6):1591–600.
[29] De Vis JB, Hendrikse J, Groenendaal F, de Vries LS, Kersbergen KJ, Benders MJ, et al. Impact of neonate haematocrit variability on the longitudinal relaxation time of blood: implications for arterial spin labelling MRI. Neuroimage Clin 2014;4:517–25.
[30] Jain V, Duda J, Avants B, Giannetta M, Xie SX, Roberts T, et al. Longitudinal reproducibility and accuracy of pseudo-continuous arterial spin-labeled perfusion MR imaging in typically developing children. Radiology 2012;263(2):527–36.
[31] Wu WC, St Lawrence KS, Licht DJ, Wang DJ. Quantification issues in arterial spin labeling perfusion magnetic resonance imaging. Top Magn Reson Imaging 2010;21(2):65–73.
[32] Harte GJ, Gray PH, Lee TC, Steer PA, Charles BG. Haemodynamic responses and population pharmacokinetics of midazolam following administration to ventilated, preterm neonates. J Paediatr Child Health 1997;33(4):335–8.